Industrial PERC+ solar cell efficiency projection towards 24%

Thorsten Dullweber, Maximilian Stöhr, Christian Kruse, Felix Haase, Birgit Beier, Philip Jäger, Verena Mertens, Robby Peibst & Rolf Brendel, Institute for Solar Energy Research Hamelin (ISFH), Emmerthal, Germany

Abstract

Monofacial passivated emitter and rear cells (PERC) and bifacial PERC+ solar cells have become the mainstream solar cell technologies in today's PV industry, with conversion efficiencies of around 22.5% being demonstrated in mass production. Ten years ago, the PV market was dominated by monofacial Al-BSF solar cells, with conversion efficiencies around 18%, while the first industrial prototype PERC cells reached 19% efficiency. This paper reviews the key technology improvements which have enabled a continuous 0.5%$_{abs}$/year increase in efficiency of industrial PERC and PERC+ cells. Most importantly, all saturation current density contributions of PERC cells have been steadily reduced, thereby enabling a noteworthy increase in V_{oc} from 620mV in 2010 to 685mV today. A breakdown of all J_o contributions of current industrial PERC+ cells is presented on the basis of actual measurements at ISFH, and a projection is provided of the improvements in J_o of industrial PERC+ cells which are feasible within the next two years, supported by published research results. These J_o values are used as input parameters for Quokka simulations of PERC+ solar cells, according to which an increase in efficiency towards 23.8% within the next two years is predicted. A main limitation of these future PERC+ cells will be the specific saturation current density $J_{o,Ag}$ = 1,400fA/cm² of the screen-printed Ag front contact. When carrier-selective poly-Si on oxide (POLO) fingers are used below the screen-printed Ag contacts, the Quokka simulations predict a further efficiency increase to 24.1% for these so-called *PERC+POLO* solar cells. The simulation results are in good agreement with published efficiencies of the first R&D-type PERC+POLO cells. However, the challenge remains of how to cost-effectively manufacture local poly-Si fingers. The local plasma-enhanced chemical vapour deposition (PECVD) of poly-Si fingers through a shadow mask is proposed as a possible manufacturing solution.

Introduction

The monofacial passivated emitter and rear cell (PERC) and bifacial PERC+ solar cell [1] have become the mainstream solar cell technologies in the PV industry, exhibiting conversion efficiencies in mass production of around 22.5% and in pilot production of up to 23.0% [2]. For more than a decade, the conversion efficiency of industrial PERC and PERC+ solar cells has continuously increased by approximately 0.5%$_{abs}$ per year [2,3]. As will be described in detail in the following section, the key technology improvements enabling steady increases in efficiency have been:

1. A change from the Al-BSF to the PERC design, applying an AlO_x/SiN surface passivation and the continuous optimization of local Al rear contacts, thereby minimizing carrier recombination at the rear ($J_{o,rear}$).
2. Continuous improvements of the phosphorus emitter, including local laser doping, thereby reducing the emitter saturation current density ($J_{o,E}$).
3. Advanced monocrystalline Cz wafers, which have only recently incorporated Ga doping, thereby enabling high and long-term-stable bulk carrier lifetimes.
4. Continuous improvement of the screen-printed front Ag fingers, with significant decreases in fingers widths over the past 10 years, thereby reducing front shadowing and front-contact recombination and enabling the contacting of advanced emitter designs.
5. The bifacial PERC+ design, which enables light harvesting from the rear side of industrial solar cells, thereby further increasing the energy yield of bifacial PV power plants. This has led to record low electricity price tenders below US$0.02/kWh in recent PV power plant auctions.

To predict future PERC and PERC+ efficiency improvements, a previous simulation study suggested that up to 24%-efficient industrial PERC cells could be developed in the future by continuous process improvements [4]. In order to suppress Ag contact recombination, the study assumed that a selective emitter with a very deep doping profile below the Ag contacts can be obtained by a deep phosphorus diffusion followed by a selective etch-back process. However, such a process combination is so far too expensive for industrial production and has therefore not yet been adapted to mass production by PERC cell manufacturers. Instead, several solar cell manufacturers fabricate selective emitters using laser doping [5]; this, however, only slightly increases the phosphorus concentration at the surface of the emitter [6], which is not sufficiently deep to have a strong effect on reducing contact recombination.

Another promising approach to achieving higher industrial cell efficiencies is the use of carrier-selective contacts by implementing a polycrystalline silicon (poly-Si) layer on a thin interfacial oxide layer, called *POLO* [7] or *TOPCon* [8] and their industrial solar cell variants, in particular *PERPoly* [9], *TOPCon* [10] and *monoPoly* [11] solar

cells. These solar cells demonstrate conversion efficiencies of around 23.0% [11] when production-type processing sequences are used. Nevertheless, the processing costs are substantially higher than those for PERC, since TOPCon-like solar cells utilize silver (Ag) contacts on both wafer sides, thus almost doubling the metallization costs compared with PERC [12]. Furthermore, the n-type Cz wafers used for TOPCon are still a bit more expensive than the p-type wafers for PERC, and the boron diffusion takes longer and hence has a lower throughput than a phosphorus diffusion [12]. These may be the reasons why the PV industry has not yet adopted TOPCon, PERPoly and monoPoly as mainstream technologies in multi-GWp production volumes.

This paper shows that the conversion efficiency of today's industrial PERC and PERC+ solar cells is still mainly limited by charge-carrier recombination, and provides a detailed up-to-date breakdown of all Jo contributions. Looking forward, near-term feasible J_o improvements are extrapolated, and the near-term efficiency potential of industrial PERC+ solar cells is simulated. A solar cell design, referred to as *PERC+POLO*, is also simulated, in which 70µm-wide poly-Si fingers located below the Ag metal contacts should drastically reduce charge-carrier recombination. The numerical simulations demonstrate an efficiency potential of up to 24.1% for PERC+POLO solar cells, assuming industrial process technologies. A very similar type of solar cell was presented in 2018 by JinkoSolar and in 2019 by LONGi Solar, with experimental conversion efficiencies of 23.9% [13] and 24.1% [14], respectively, both obtained in R&D. However, JinkoSolar and LONGi did not present any process technology information about the poly-Si finger formation for these solar cells.

A very cost-efficient PERC+POLO manufacturing process is proposed, which implements the well-established PERC+ process and incorporates only one additional process step, specifically the plasma-enhanced chemical vapour deposition (PECVD) of a-Si fingers through a shadow mask. This paper is a shortened version of a recent publication [3], in which details related to the proposed PERC+POLO process sequence, and promising preliminary results of experimental 70µm-wide poly-Si fingers deposited by PECVD through a shadow mask, can be found.

"The conversion efficiency of today's industrial PERC and PERC+ solar cells is still mainly limited by charge-carrier recombination."

J_o analysis of past, present and future PERC and PERC+ solar cells

In order to predict future technology developments, a common approach in semiconductor technology is to try to extrapolate the technology trends from the past into the future, as (for example) in the case of the regularly published ITRPV Roadmap [15]. Fig. 1(a) shows the record efficiencies of industrial PERC solar cells from 2010 till 2019. The best PERC+ cell efficiencies since their first publication in 2015 [1] are shown as well, with front-side efficiencies

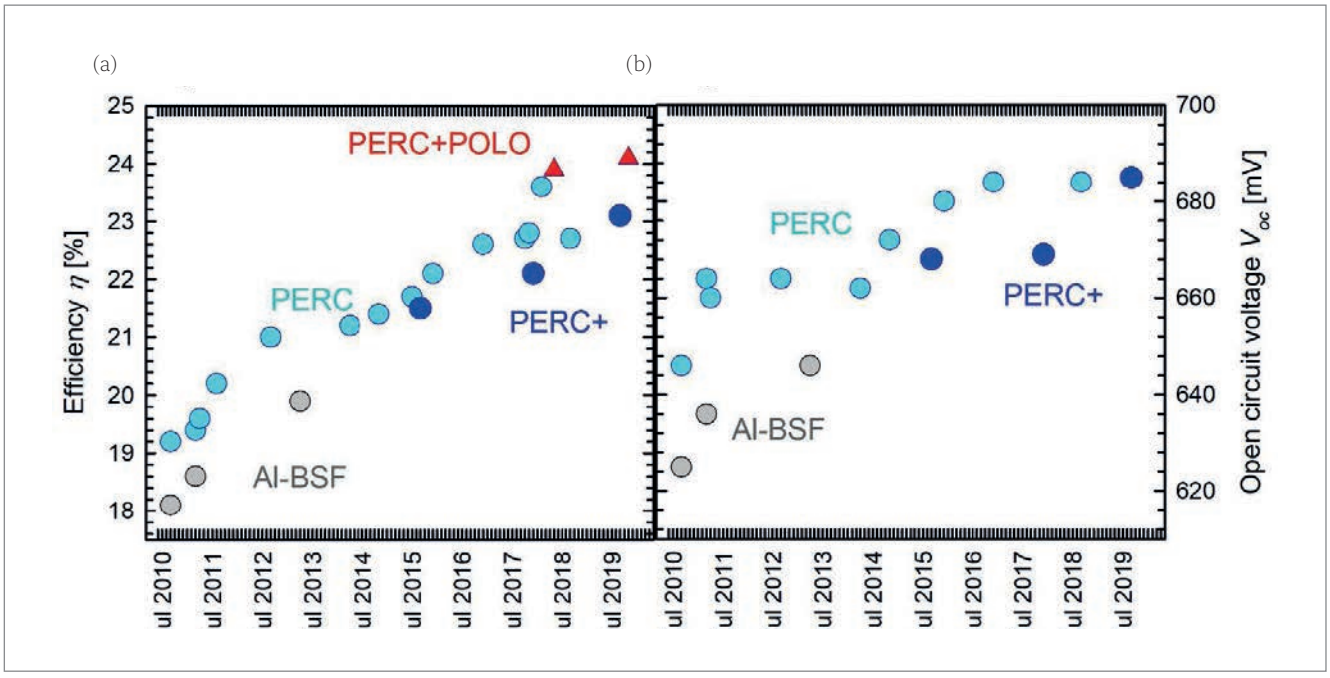

Figure 1. (a) The record efficiency (light blue dots) of industrial PERC solar cells has constantly increased by about 0.5%$_{abs}$/year from 19.2% in 2010 up to 23.6% in 2019. The best bifacial PERC+ cells (dark blue dots) exhibit similar efficiencies to those of the monofacial PERC cells. The initial R&D-type PERC+POLO cells (red triangles) achieve efficiencies of around 24%. (b) The V_{oc} has improved from 625mV for Al-BSF cells (grey dots) in 2010, to 685mV for industrial PERC+ cells in 2019, thus being a main contributor to the higher conversion efficiencies. Unfortunately, the V_{oc} values of the record PERC+POLO cells have not been published (but simulated values are shown later in Fig. 4). The main reasons for the 5% $_{abs}$ efficiency improvement during the past nine years are explained later in Fig. 2 and Table 1, which also provide a forecast for 2022. (Note that this figure is an updated version of the one given in Dullweber [16], and now includes data from other publications [1,2,13,14,39].)

	2010 Al-BSF	Technology improvement	2019 PERC/PERC+	2022 PERC+	2022 PERC+POLO
$f_{Al} \times J_{0,Al\text{-}BSF}$	100% × 300fA/cm²	PERC	4% × 400fA/cm²	1% × 400fA/cm²	1% × 400fA/cm²
$J_{0,AlOx/SiN}$	N/A	PERC	12fA/cm²	1fA/cm²	1fA/cm²
$J_{0,rear}$	300fA/cm²		28fA/cm²	5fA/cm²	5fA/cm²
$J_{0,E}$	100fA/cm²	In situ / ex situ oxidation, LDSE	30fA/cm²	22fA/cm²	22fA/cm²
$f_{Ag} \times J_{0,Ag}$	7% × 1,400fA/cm²	Fine-line Ag print, 0BB	3% × 1,400fA/cm²	2% × 1,400fA/cm²	2% × 35fA/cm²
$J_{0,front}$	198fA/cm²		72fA/cm²	50fA/cm²	23fA/cm²
$J_{0,bulk}$	80fA/cm²	Low O_i, Ga	30fA/cm²	8fA/cm²	8fA/cm²
$J_{0,total}$	578fA/cm²		130fA/cm²	63fA/cm²	36fA/cm²
Calc. V_{oc}	636mV		678mV	696mV	711mV
J_{sc}	37.0mA/cm²	PERC, fine-line Ag print	41.0mA/cm²	41.0mA/cm²	41.0mA/cm²
Bifaciality	0%	PERC+	80%	90%	90%

Table 1. Detailed breakdown of the contributions to the reduction of the $J_{0,total}$ from 578fA/cm² in 2010 to 130fA/cm² in 2019, which enabled a large increase in V_{oc} as the main driver for the efficiency improvements shown in Fig. 1. Furthermore, a projection is provided for the expected J_0 contributions of PERC+ and PERC+POLO cells in 2022 (which are subsequently used in the Quokka simulations in Fig. 4). The individual J_0 values were either measured at ISFH or taken from the literature.

comparable to monofacial PERC cells. As a reference, the published efficiencies of full-area Al-BSF solar cells are shown, which, however, have been phased out of industrial mass production in favour of PERC and PERC+. The R&D-type PERC+POLO cells of Jinko and LONGi, yielding efficiencies of around 24% [13,14], are also included in Fig. 1(a).

Whereas a typical industrial Al-BSF solar cell in the year 2010 had an efficiency of around 17.5%, today's industrial PERC and bifacial PERC+ solar cells exhibit average conversion efficiencies of around 22.5% in mass production, approaching the record PERC efficiencies of around 23% displayed in Fig. 1(a). This corresponds to an efficiency increase of $5\%_{abs}$ of industrial silicon solar cells within nine years, and a fairly constant efficiency learning rate of around $0.5\%_{abs}$/year during the last decade.

Fig. 1(b) presents the historic trend of the open-circuit voltage V_{oc} of Al-BSF, PERC and PERC+ solar cells, and reveals an increase from 625mV in 2010 to 685mV in 2019, thus indicating it to be a main contributor to the $5\%_{abs}$ efficiency increase shown in Fig. 1(a). The PERC design led to an increase in the V_{oc} of Al-BSF cells of approximately 20mV. Further increases in the V_{oc} of PERC cells mainly originated from improved emitter doping profiles and reduced Ag front-contact area (as explained later in Table 1). Because of their similar device structure, PERC and PERC+ solar cells exhibit very similar V_{oc} values, as can be observed in Fig. 1(b). Unfortunately, the V_{oc} values of the 24%-efficient PERC+POLO cells have not been published (but are simulated to be around 700mV, as will be seen later in Fig. 4). The V_{oc} improvements, together with reduced Ag front-grid shadowing and improved rear optics of PERC, also significantly increased the short-circuit current density J_{sc} from 37mA/cm² in 2010 [17] to 41mA/cm² in 2019 [2]; this too played a big part in the increased conversion efficiency illustrated in Fig. 1(a).

Table 1 lists the most important technology improvements from typical Al-BSF cells in 2010 to typical monofacial PERC and bifacial PERC+ cells in 2019, enabling the continuous increases in the efficiency and V_{oc} of industrial silicon solar cells, as shown in Fig. 1. Since PERC and PERC+ cells exhibit almost identical saturation current density J_0 values because of their very similar device structure, their J_0 values for 2019 are shown in the combined column '2019 PERC/PERC+' in Table 1. The J_0 values stated in Table 1 are either measured for industry-typical PERC and PERC+ cells processed at ISFH, or taken from the literature as indicated in the following paragraphs. Two further columns have been added in Table 1, extrapolating the future J_0 reduction and V_{oc} improvement potential for PERC+ and PERC+POLO cells.

The key improvement when moving from Al-BSF cells to PERC cells was the reduction in area fraction f_{Al} of the aluminium rear contacts from 100% to around 4% today, thereby drastically minimizing charge-carrier recombination at the rear metal contact. Fig. 2 shows two scanning electron microscopy (SEM) cross-section images for (a) a 19.4%-efficient ISFH PERC cell in 2010 [17], and (b) a 22.3%-efficient ISFH PERC+ cell in 2019. As can be seen, the early PERC cells had around 100µm-wide line-shaped alloyed Al contacts, which contacted around 10% of the rear area.

"The key improvement when moving from Al-BSF cells to PERC cells was the reduction in area fraction of the aluminium rear contacts from 100% to around 4% today."

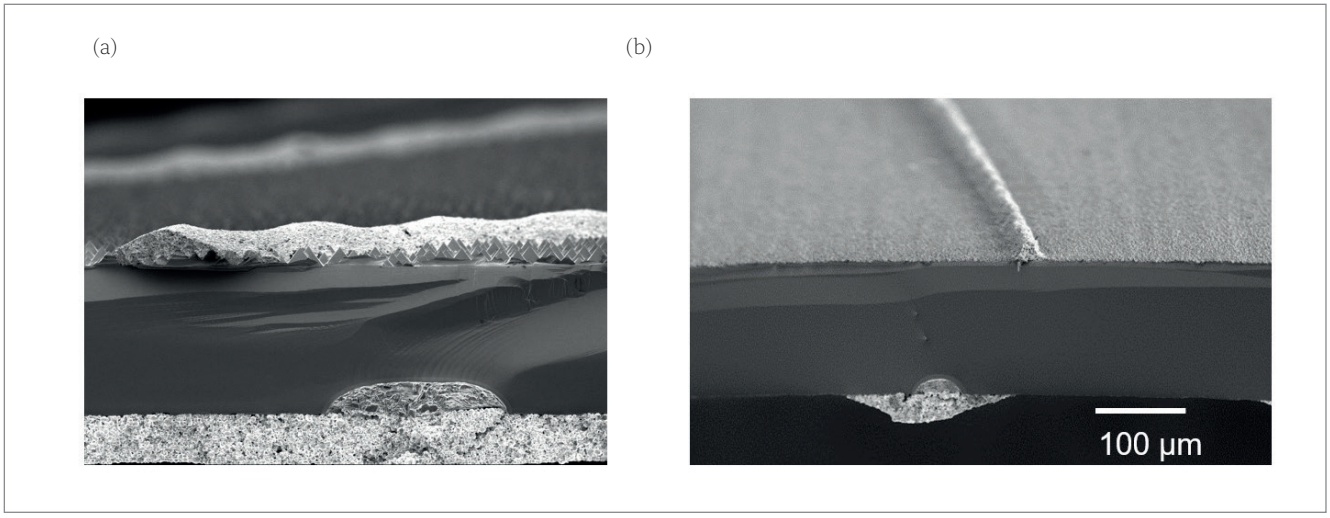

Figure 2. Scanning electron microscopy (SEM) images of: (a) the 19.4%-efficient ISFH PERC record cell in 2011 (see Fig. 1); and (b) a 22.3%-efficient ISFH bifacial PERC+ solar cell from 2019. Whereas the Si wafer thickness has remained constant at about 180µm, the Ag finger widths have been reduced from around 100µm in 2010 to around 35µm in 2019, thus minimizing light reflection and front-contact recombination. The Al-BSF contact-area fraction has been reduced from 100% for Al-BSF cells to around 10% for the early PERC cells in 2010, and to around 4% for today's PERC+ solar cells. Although the *y* axis is the same for both SEM images, the *x* axis in image (a) is stretched by a factor of 1.4, since the PERC cell has been broken in a 45° angle to the metal fingers. In (b), the cell has been broken in a 90° angle to the Ag fingers.

By improving the laser contact opening pattern and the Al paste chemistry it was possible to further reduce the Al contact-area fraction to around 4% while maintaining a well-alloyed aluminium back surface field (Al-BSF), enabling fairly low $J_{o,Al\text{-}BSF}$ values around 400fA/cm², as described in the review in Dullweber [16], as well as according to ISFH internal measurements. Additionally, the Al fingers of PERC+ cells limit the diffusion of Si into the Al paste during firing and hence slightly deeper Al-BSFs and lower $J_{o,Al\text{-}BSF}$ values [18] may be obtained. In any case, the specific $J_{o,Al\text{-}BSF}$ = 400fA/cm² of PERC and PERC+ is only slightly higher than that for full-area Al-BSF contacts with $J_{o,Al\text{-}BSF}$ values around 300fA/cm² [17]. Hence, the total area-weighted J_o contribution of the Al rear contacts has decreased from 300fA/cm² in 2010 to just 16fA/cm² in 2019.

In the next few years, it is expected that

improved LCO geometries and Al pastes will further reduce the Al contact-area fraction to around 1% without increasing the specific $J_{o,Al\text{-}BSF}$, as already demonstrated in Peng et al. [19] and Tsuji et al. [20], thereby minimizing the area-weighted J_o contribution of the Al rear contacts to just 4fA/cm², as shown in Table 1. At the same time, the AlO_x/SiN_y rear passivation covering almost 100% of the PERC+ rear side contributes a $J_{o,AlOx/SiN}$ of only 12fA/cm² to the total J_o [21] as a result of its excellent passivation properties. It is expected that $J_{o,AlOx/SiN}$ will be reduced to 1fA/cm² in the next few years by continuous process optimization, as this value has already been measured on test structures at ISFH. Accordingly, the total rear-side saturation current density $J_{o,rear}$, which is the sum of the area-weighted contributions of $J_{o,Al\text{-}BSF}$ and $J_{o,AlOx/SiN}$, has dropped from 300fA/cm² in 2010 to 28fA/cm² in 2019, and is expected to further decrease to just 5fA/cm² in 2022.

Another important contribution to increases in efficiency and V_{oc} has been the reduction of the emitter saturation current density $J_{o,E}$ from around 100fA/cm² [22,23] back in 2010 to today's values of around 30fA/cm² [24,25] by developing advanced emitter doping profiles with reduced phosphorus surface concentrations through applying techniques such as in situ [26–28] and ex situ oxidation [25,29]. The advanced diffusion processes reduce $J_{o,E}$ while maintaining an emitter sheet resistance below 150Ω/sq., which allows a wide spacing, greater than 1mm, of the Ag front-contact fingers. Just as important were new developments, such as improved Ag pastes and laser-doped selective emitters (LDSE) [5,6], which enabled the electrical contacting of the advanced doping profiles. It is expected that this trend will continue and that $J_{o,E}$ values of 22fA/cm² will be obtained in production in the coming years, since such low $J_{o,E}$ values have already been published in R&D [24,25].

One of the most important contributions to increased crystalline silicon solar cell conversion efficiencies in the last few decades has been the continuous improvement of the front Ag pastes. Improved Ag paste chemistries have made possible much narrower Ag finger widths [30], thus reducing the optical shadowing loss and metal contact charge-carrier recombination loss. Improved Ag pastes have also allowed the contacting of lightly doped emitters as stated earlier. The two SEM images in Fig. 2 demonstrate the huge progress in reducing the front Ag finger widths from approximately 100µm in 2010 to around 35µm in 2019, according to Lorenz et al. [30]. Consequently, the metallization area fraction f_{Ag} of the Ag front fingers has fallen from 5% in 2010 to around 2.5% in 2019.

> "Another promising approach to reducing metal contact recombination is the use of carrier-selective contacts, which entails the application of polycrystalline silicon on thin interfacial oxide."

Simultaneously, the busbar design has also changed during the past nine years. Whereas in 2010, typically three busbars were printed with fire-through Ag pastes, contacting around 2% of the front surface, today's PERC+ cells often utilize non-fire-through busbar pastes and/or advanced multi-busbar designs [31], which cover less than 0.5% of the wafer front surface. In consequence, the total contacted area fraction f_{Ag} (Ag fingers and busbars) has decreased from around 7% in 2010 to around 3% in 2019 (see Table 1).

For the front Ag contacts, a specific $J_{o,Ag}$ = 1,400fA/cm² is determined by a detailed carrier lifetime measurement and subsequent numerical modelling using Quokka. This value is within the range of previously reported $J_{o,Ag}$ values, specifically from 200 to 2500fA/cm² [29,32–34], which depend in particular on the sheet resistance and doping profile of the phosphorus emitter. Assuming a similar $J_{o,Ag}$ of up to 1,400fA/cm² back in 2010, the area-weighted J_o contribution of the Ag front contacts

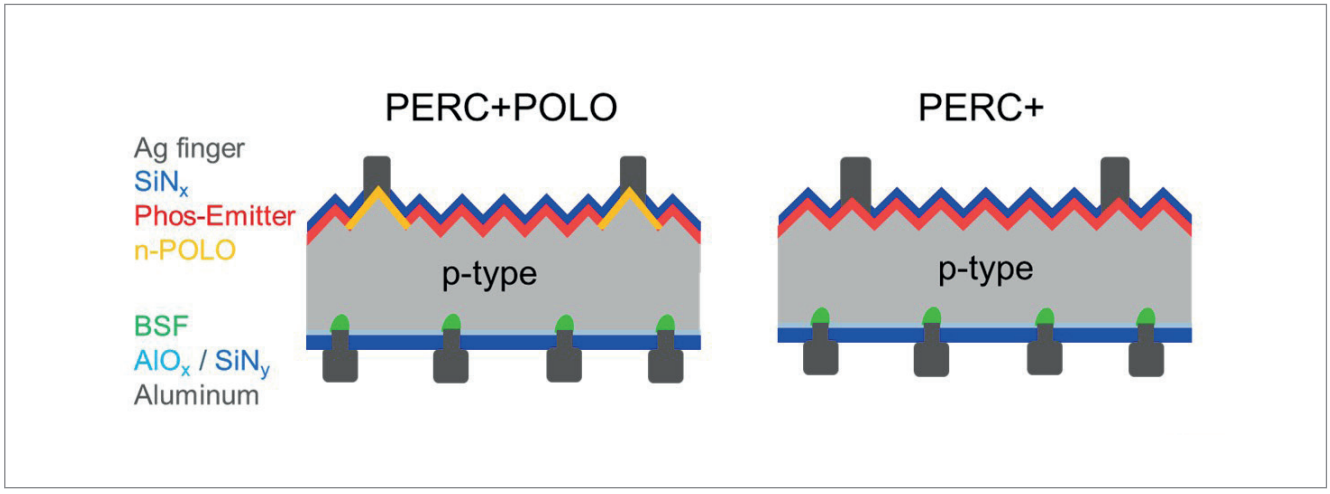

Figure 3. Schematic drawings of PERC+POLO and PERC+ solar cells. The poly-Si on oxide (POLO) finger below the Ag finger drastically minimizes the front-contact recombination.

has decreased from 98fA/cm² in 2010 to 42fA/cm² in 2019, as indicated in Table 1. The possibility of further reductions in the Ag finger width towards 25µm in the next few years [30] is expected, hence further reducing the contacted area fraction f_{Ag} to an anticipated 2% in 2022.

It is quite challenging, however, to reduce the high $J_{o,Ag}$ of 1,400fA/cm². One solution to suppress Ag contact recombination is the use of selective emitters with a very deep doping profile below the Ag contacts [29]. Unfortunately, the industry-typical laser-doped selective emitter forms only a shallow emitter, since the higher laser intensities required for deep doping cause melting of the silicon pyramids [6]. Other techniques, such as deep phosphorus diffusion followed by a selective etch-back process [22], are likely to be too expensive for industrial production and hence have not yet been adapted to mass production.

Another promising approach to reducing metal contact recombination is the use of carrier-selective contacts, which entails the application of polycrystalline silicon on thin interfacial oxide, referred to as *POLO* [7] or *TOPCon* [8] and their industrial solar cell variants. It has been shown that the carrier recombination at the screen-printed Ag metal contacts can be minimized to 35fA/cm² with carrier-selective poly-Si contacts [35]. When weighted with the contact-area fraction of 2%, the recombination at the Ag/poly-Si contact is well below 1fA/cm². Hence, in Table 1 the column 'PERC+POLO 2022' has been introduced on the right, where it is suggested to insert a poly-Si finger below the Ag finger of a PERC+ solar cell, similarly to Jin [13] and Fan et al. [14].

A schematic drawing of the PERC+POLO cell in comparison to an industry-typical PERC+ cell is shown in Fig. 3. The total front-side saturation current density $J_{o,front}$, which is the sum of the area-weighted contributions of $J_{o,Ag}$ and $J_{o,E}$, has fallen from 198fA/cm² in 2010 to 72fA/cm² in 2019, thus making it the main V_{oc} limitation of today's PERC and PERC+ solar cells. Advanced emitters and the PERC+POLO cell design are expected to reduce $J_{o,front}$ to 23fA/cm² in 2022.

Finally, the saturation current density $J_{o,bulk}$ of p-type Czochralski (Cz) silicon wafer material has also been reduced, from around 80fA/cm² [36] in 2010 to around 30fA/cm² in 2019 [37], by improving the wafer quality, by reducing the oxygen content and by regeneration procedures minimizing boron–oxygen defect recombination (see, for example, the review in Dullweber [38]). Here, $J_{o,bulk}$ is reported at a carrier density of 1×10^{15}cm^{-3}, which corresponds to V_{oc} conditions. The $J_{o,bulk}$ values at maximum power point are slightly higher because of the injection dependence of the bulk carrier lifetime. In the past decade, the p-type Cz wafer resistivity has decreased from around 2Ωcm in 2010 to around 1Ωcm in 2019 [37], which enables a wider Al finger spacing of greater than 1mm and hence an increased bifaciality of PERC+ solar cells. It is expected that the improvement of the p-type Cz wafer material will continue and enable $J_{o,bulk}$ values as low as 8fA/cm², as evidenced by today's best R&D Cz wafers utilizing Ga doping or extremely low oxygen concentrations [37].

Adding up the individual area-weighted saturation current density contributions in Table 1 by applying Equation 1 results in a total $J_{o,total}$ = 578fA/cm² for the Al-BSF cell in 2010.

$$J_{0,\text{total}} = f_{Ag}\times J_{0,Ag} + \left(1-f_{Ag}\right)\times J_{0,E} + J_{0,\text{bulk}} + f_{Al}\times J_{0,Al} + \left(1-f_{Al}\right)\times J_{0,Al} \quad (1)$$

$$V_{oc} = \frac{nkT}{q}\times \ln\left(\frac{J_{sc}}{J_{0,\text{total}}}\right) \quad (2)$$

When a one-diode model is applied according to Equation 2 with ideality factor n = 1 and short-circuit current density J_{sc} = 37mA/cm² [17], this $J_{o,total}$ value corresponds to a V_{oc} of 636mV for the Al-BSF cell, which closely agrees with measured I–V parameters at that time [17].

For the PERC+ cell in 2019, a $J_{o,total}$ value of 130fA/cm² is obtained, corresponding to a V_{oc} of 678mV when J_{sc} = 41mA/cm² is assumed [2]. This number is not far off the V_{oc} of around 680mV of today's typical PERC+ cells [2]. It should be noted that the largest $J_{o,total}$ contribution of 42fA/cm² originates from the recombination at the Ag front contacts. ISFH's extrapolation of the PERC+ parameters to 2022 predicts a $J_{o,total}$ value of 63fA/cm², corresponding to a calculated V_{oc} of 696mV, which is limited, again, mainly by $f_{Ag}\times J_{o,Ag}$ = 28fA/cm².

Finally, the extrapolation to 2022 for the PERC+POLO cell results in the smallest $J_{o,total}$ value of 36fA/cm², corresponding to a calculated V_{oc} of 711mV. Experimental evidence for this fairly high calculated V_{oc} of PERC+POLO cells is given by measured implied open-circuit voltages iV_{oc} of up to 712mV [25] for PERC+ solar cells processed at ISFH without metal contacts; this corresponds to a total $J_{o,iVoc}$ = 35fA/cm². According to Table 1, the iV_{oc} values of PERC+ test structures differ from the V_{oc} values of PERC+POLO cells mainly by the $f_{Al}\times J_{o,Al\text{-}BSF}$ contribution, which is only 4fA/cm² in the 2022 scenarios. Since $f_{Ag}\times J_{o,Ag}$ for PERC+POLO is less than 1fA/cm² and the $f_{Al}\times J_{o,Al\text{-}BSF}$ is only 4fA/cm², it is expected that the $J_{o,total}$ for PERC+POLO will only increase by 5fA/cm², from 31 to 36fA/cm², after metallization; hence, the cell V_{oc} for PERC+POLO will be close to the iV_{oc} of 712mV of PERC+ cells without metal contacts [25].

Another important improvement which significantly increases the energy yield of PERC solar cells and modules is the introduction of bifacial PERC solar cells called *PERC+* [1], where an

"Quokka simulations confirm that PERC+POLO cells yield higher V_{oc} values and higher conversion efficiencies, compared with PERC+ solar cells."

Parameter	Value
Wafer resistivity	0.9Ωcm
Wafer thickness	170µm
Front-contact shadowing	3.0%
Emitter sheet resistance R_{sh}	133Ω/sq.
Specific contact resistance, front	1.5mΩcm²
Specific contact resistance, rear	1.3mΩcm²

Table 2. Input parameters used for the Quokka simulations in Fig. 4, as measured at ISFH. The J_o and f values for the different PERC+ and PERC+POLO scenarios were taken from Table 1.

Al finger grid is applied on the rear side. Whereas the full-area Al-BSF cells in 2010, as well as the first commercial PERC cells, were monofacial with 0% bifaciality, today's PERC+ solar cells exhibit a bifaciality of up to 80% [1,2,16]. Between now and 2022, the bifaciality of PERC+ solar cells is expected to increase to 90% through further reductions of the Al finger width in combination with multi-busbar module designs as outlined in Dullweber et al. [39].

Quokka simulations of the near-term PERC+ efficiency potential

The conversion efficiency potential of PERC+ and PERC+POLO solar cells is assessed in detail by means of numerical simulations by applying the conductive boundary model [40] as implemented in the Quokka software [41]. Two topical scenarios are simulated for PERC+ and PERC+POLO cells. The 'PERC+ 2019' scenario uses all J_o and f parameters as stated in the '2019 PERC/PERC+' column in Table 1. The 'PERC+POLO 2019' scenario also applies the J_o and f parameters as stated in the '2019 PERC/PERC+' column in Table 1, except for the $J_{o,Ag}$ value, where 35fA/cm² is used for the Ag on POLO contact instead of 1,400fA/cm² for the Ag on phosphorus emitter contact. All other input parameters for both scenarios are given in Table 2 and were measured at ISFH. The 'PERC+POLO 2019' scenario assumes 90µm-wide poly-Si fingers in order to account for possible misalignment between poly-Si structuring and Ag screen printing. The optical absorption of the 90µm-wide poly-Si fingers is included in the 'PERC+POLO 2019' scenario using a ray-tracing approach with optical constants according to Reiter et al. [42] and Min et al. [43].

	η [%]	V_{oc} [mV]	J_{sc} [mA/cm²]	FF [%]
ISFH PERC+ cell	22.3	683	40.4	80.8
PERC+ 2019 Quokka	22.7	682	40.8	81.8
PERC+ 2022 Quokka	23.8	697	41.3	82.5
PERC+POLO 2022 Quokka	24.1	712	40.9	82.8

Table 3. *I–V* parameters for an industrial PERC+ cell processed at ISFH in 2019 compared with those for the various simulated scenarios using the input parameters from Tables 1 and 2.

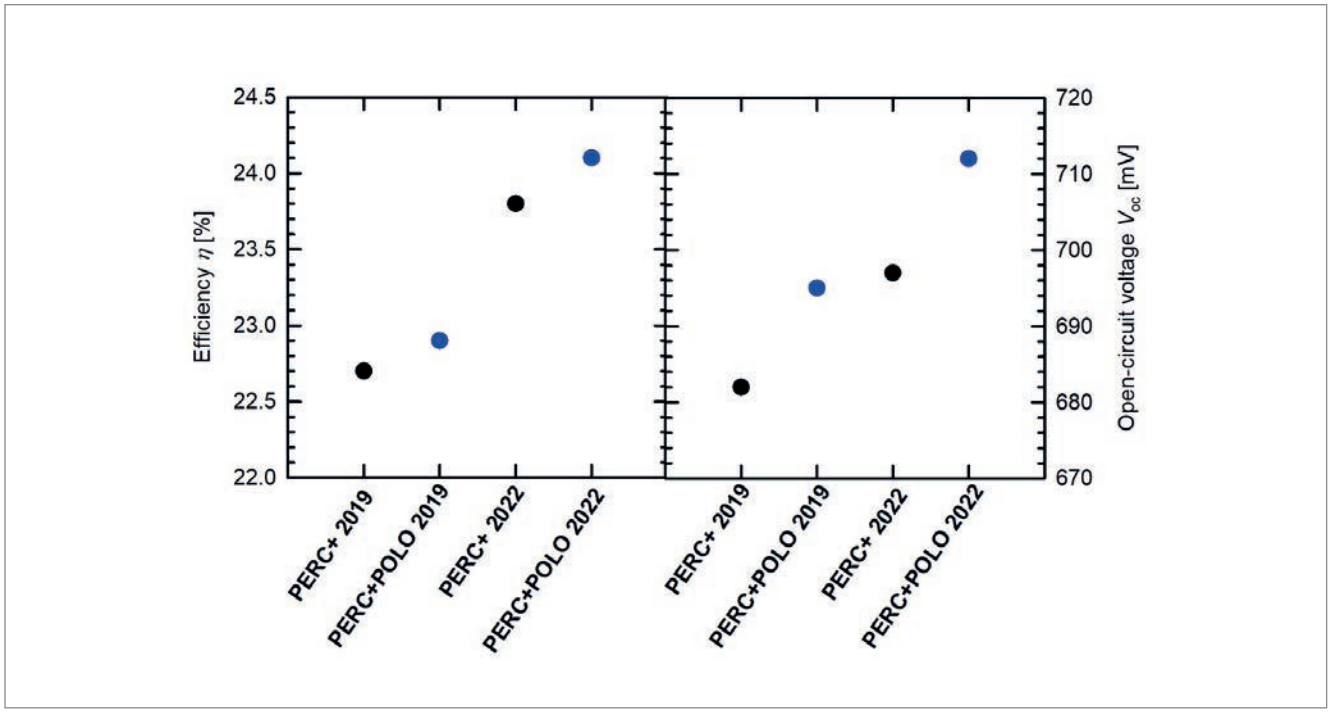

Figure 4. Simulated conversion efficiencies of PERC+ and PERC+POLO solar cells from using the Quokka software and typical PERC+ and POLO input parameters as measured in 2019 and as expected in 2022 (see Tables 1 and 2). The application of POLO contacts increases the efficiency η by up to 0.3%$_{abs}$, towards 24.1%, and V_{oc} by up to 15mV, towards 712mV.

Table 3 lists the simulated current–voltage (*I–V*) parameters of the 'PERC+ 2019' scenario with a conversion efficiency η = 22.7%, which is in good agreement with both the industry status and the PERC+ cell in Table 3 processed at ISFH with η = 22.3% efficiency measured in-house. As shown in Fig. 4, the 'PERC+POLO 2019' simulation demonstrates 0.2%$_{abs}$ higher efficiencies and yields 22.9%. As a result of the Ag contact recombination being practically eliminated, the V_{oc} increases from 682mV for PERC+ to 695mV for PERC+POLO.

In a second set of simulations, it is assumed that within the next three years the PERC+ J_o and f parameters will be further improved, as indicated in the '2022 PERC+' column of Table 1; accordingly, the simulated 'PERC+ 2022' efficiency increases to 23.8% and the V_{oc} to 697mV. For the 'PERC+POLO 2022' scenario, the J_o and f parameters given in the '2022 PERC+POLO' column in Table 1 are assumed; these quantities are identical to those for 'PERC+ in 2022', except for the much lower $J_{o,Ag}$ value of the POLO contact.

In addition, it is assumed that it will be possible to reduce the poly-Si finger width to 70µm as a result of improved alignment between poly-Si structuring and Ag screen printing; accordingly, the 'PERC+POLO 2022' simulation achieves the highest conversion efficiency of 24.1% and the highest V_{oc} of 712mV. Again, this high simulated V_{oc} is supported by ISFH's experimentally highest PERC+ implied open-circuit voltage iV_{oc} of 712mV [25]. However, as shown in Table 3, the J_{sc} of the simulated PERC+POLO 2022 cell is 0.4mA/cm² lower than that of the PERC+ 2022 cell because of absorption in the 70µm poly-Si fingers.

Conclusion

In the past decade, almost all contributions to saturation current density J_o in industrial silicon solar cells have been steadily reduced through the use of new process technologies, such as the PERC concept with AlO_x/SiN_y rear passivation and LCOs, improved emitter doping profiles by in situ and ex situ oxidation, continuous improvements to Ag pastes enabling narrower Ag finger widths, and so on. The reduction in J_o from around 578fA/cm² in 2010 to around 100–150fA/cm² today was a key contribution to increasing the conversion efficiency of 17.5% of Al-BSF cells in 2010 towards 22.5% of today's mass-produced PERC and PERC+ solar cells.

A J_o analysis of current industrial PERC+ solar cells reveals all the individual J_o contributions. Assuming realistic evolutionary improvements, such as further reduced emitter and wafer bulk J_o values, a near-term efficiency potential of up to 23.8% for industrial PERC+ solar cells was simulated. Carrier recombination at the Ag front contact is the biggest contribution to the total $J_{o,total}$ value, thus limiting the V_{oc} to below 700mV. Hence, the PERC+POLO cell concept was simulated, which utilizes poly-Si fingers below the Ag contact, thereby potentially minimizing the area-weighted $J_{o,Ag}$ contribution to below 1fA/cm². Quokka simulations confirm that PERC+POLO cells yield 15mV higher V_{oc} values, of up to 712mV, and 0.3%$_{abs}$ higher conversion efficiencies, of up to 24.1%, compared with PERC+ solar cells. These simulations are supported experimentally by a measured implied open-circuit voltage iV_{oc} = 712mV of PERC+ cell precursors processed at ISFH without metal contacts, as well as by the 24.1%-efficient R&D-type PERC+POLO solar cell published by LONGi.

Because of the relatively small efficiency gain of PERC+POLO over PERC+, in order to be cost effective a very lean manufacturing process flow is proposed for PERC+POLO in which there is only one additional process step compared with PERC+, namely the local deposition of poly-Si fingers by PECVD through a shadow mask. In preliminary experimental tests, the narrowest poly-Si finger widths of 70µm were demonstrated, more details of which can be found in Dullweber et al. [3].

Acknowledgements

The authors gratefully acknowledge the support of the German Federal Ministry for Economic Affairs and Energy under the contracts 0324294C and 0324246B.

References

[1] Dullweber, T. et al. 2016, "PERC+: Industrial PERC solar cells with rear Al grid enabling bifaciality and reduced Al paste consumption", *Prog. Photovolt: Res. Appl.,* Vol. 24, pp. 1487–1498.

[2] Stenzel, F. et al. 2019, "Exceeding 23% and mass production of p-Cz Quantum bifacial solar cells", *Proc. 36th EU PVSEC*, Marseille, France, pp. 96–99.

[3] Dullweber, T. et al. 2020, "Evolutionary PERC+ solar cell efficiency projection towards 24% evaluating shadow-mask-deposited poly-Si fingers below the Ag front contact as next improvement step", *Sol. Energy Mater. Sol. Cells,* Vol. 212, 110586.

[4] Min, B. et al. 2017, "A roadmap toward 24% efficient PERC solar cells in industrial mass production", *IEEE J. Photovolt.*, Vol. 7, pp. 1541–1550.

[5] Eisele, S.J. et al. 2009, "18.9% efficient full area laser doped silicon solar cell", *Appl. Phys. Lett.,* Vol. 95, 133501.

[6] Lohmüller, S. et al. 2017, "Key aspects for fabrication of p-type Cz-Si PERC solar cells exceeding 22% conversion efficiency", *Proc. 33rd EU PVSEC,* Amsterdam, The Netherlands, pp. 406–412.

[7] Brendel, R. et al. 2013, "Recent progress and options for future crystalline silicon solar cells", *Proc. 28th EU PVSEC*, Paris, France, pp. 676–690.

[8] Richter, A. et al. 2017, "N-type Si solar cells with passivating electron contact: Identifying sources for efficiency limitations by wafer thickness and resistivity variation", *Sol. Energy Mater. Sol. Cells,* Vol. 173, pp. 96–105.

[9] Stodolny, M.K. et al. 2016, "N-type polysilicon passivating contact for industrial bifacial n-type solar cells", *Sol. Energy Mater. Sol. Cells,* Vol. 158, pp. 24–28.
[10] Feldmann, F. et al. 2019, "Large area TOPCon cells realized by a PECVD tube process", *Proc. 36th EU PVSEC*, Marseille, France, pp. 304–308.
[11] Nandakumar, N. et al. 2019, "Approaching 23% with large area monoPoly cells using screen printed and fired rear passivating contacts fabricated by inline PECVD", *Prog. Photovolt: Res. Appl.,* Vol. 27, pp. 107–112.
[12] Deng, W. et al. 2019, "The influence of diffusion condition to passivation quality of SiOx/poly-silicon layer", *Proc. 36th EU PVSEC*, Marseille, France, pp. 259–261.
[13] Jin, H. 2018, Presentation at 12th SNEC Int. PV Power Gen. Conf., Shanghai, China.
[14] Fan, J. et al. 2019, "The roadmap to > 24% of PERC", *Proc. 29th Internat. PVSEC*, Xi'an, China, pp. 1444–1446.
[15] ITRPV 2019, "International technology roadmap for photovoltaic (ITRPV): Results 2018", 10th edn (Mar.) [https://itrpv.vdma.org/en/].
[16] Dullweber, T. 2020, "High efficiency industrial PERC solar cells for monofacial and bifacial applications", in *High-Efficient Low-Cost Photovoltaics,* Petrova-Koch, V., Hezel, R. & Goetzberger, A., Eds. Springer Nature Switzerland AG, pp. 65 – 94.
[17] Dullweber, T. et al. 2012, "Towards 20% efficient large-area screen-printed rear-passivated silicon solar cells", *Prog. Photovolt: Res. Appl.,* Vol. 20, pp. 630–638.
[18] Kranz, C. et al. 2016, "Void formation in screen-printed local aluminum contacts modeled by surface energy minimization", *Sol. Energy Mat. Sol. Cells,* Vol. 158, pp. 11–18.
[19] Peng, Z.W. et al. 2019, "Industrial screen-printed n-PERT-RJ solar cells: Efficiencies beyond 22% and open-circuit voltages approaching 700 mV", *IEEE J. Photovolt.,* Vol. 9, pp. 1166–1174.
[20] Tsuji, K. et al. 2019, "Fine line Al printing on narrow point contact opening for front side metallization", *AIP Conf. Proc.*, Vol. 2147, 040019.
[21] Kranz, C. et al. 2012, "Impact of the rear surface roughness on industrial-type PERC solar cells", *Proc. 27th EU PVSEC*, Frankfurt, Germany, pp. 557–560.
[22] Hahn, G. 2010, "Status of selective emitter technology", *Proc. 25th EU PVSEC*, Valencia, Spain, pp. 1091–1096.
[23] Dullweber, T. et al. 2013, "Ion-implanted PERC solar cells with Al_2O_3/SiN_x rear passivation", *Energy Procedia,* Vol. 38, pp. 430–435.
[24] Deng, W. et al. 2017, "22.61 % efficient fully

screen printed PERC solar cell", *Proc. 44th IEEE PVSC*, Washington DC, USA, pp. 2220–2226.
[25] Jäger, P., Baumann, U. & Dullweber, T. 2019, "Impact of the thermal budget of the emitter formation on the pFF of PERC+ solar cells", *AIP Conf. Proc.,* Vol. 2147, 140005.
[26] Kimmerle, A. et al. 2013, "Simplified front surface field formation for back contacted silicon solar cells", *Energy Procedia,* Vol. 38, pp. 278–282.
[27] Piechulla, A. et al. 2015, "Low pressure diffusions for high quality emitter formation in advanced p- and n-type solar cells", *Proc. 31st EU PVSEC,* Hamburg, Germany, pp. 420–424.
[28] Dullweber, T. et al. 2017, "Emitter saturation current densities of 22 fA/cm^2 applied to industrial PERC solar cells approaching 22% conversion efficiency", *Prog. Photovolt: Res. Appl.,* Vol. 25, pp. 509–514.
[29] Cuevas, A. et al. 1996, "Surface recombination velocity of highly doped n-type silicon", *J. Appl. Phys.,* Vol. 80, pp. 3370–3375.
[30] Lorenz, A. et al. 2018, "Screen printed thick film metallization of silicon solar cells – Recent developments and future perspectives", *Proc. 35th EU PVSEC*, Brussels, Belgium, pp. 819–824.
[31] Braun, S. et al. 2013, "The multi-busbar design: An overview", *Energy Procedia,* Vol. 43, pp. 86–92.
[32] Hannebauer, H. et al. 2012, "Analysis of the emitter saturation current density of industrial type silver screen-printed front contacts", *Proc. 27th EU PVSEC,* Frankfurt, Germany, pp. 1360–1363.
[33] Ye, F. et al. 2016, "22.13% efficient industrial p-type mono PERC solar cell", *Proc. 43rd IEEE PVSC,* Portland, Oregon, USA, pp. 3360–3365.
[34] Shanmugam, V. et al. 2016, "Impact of the phosphorus emitter doping profile on metal contact recombination of silicon wafer solar cells", *Sol. Energy Mater. Sol. Cells,* Vol. 147, pp. 171–176.
[35] Padhamnath, P. et al. 2019, "Metal contact recombination in monoPoly™ solar cells with screen-printed & fire-through contacts", *Sol. Energy Mater. Sol. Cells*, Vol. 192, pp. 109–116.
[36] Dullweber, T. et al. 2013, "Silicon wafer material options for highly efficient p-type PERC solar cells", *Proc. 39th IEEE PVSC,* Tampa, Florida, USA, pp. 3074–3078.
[37] Lim, B. 2018, "LID-free PERC+ cells with stable efficiencies up to 22.1%", *Proc. 35th EU PVSEC,* Brussels, Belgium, pp. 359–365.
[38] Dullweber, T. & Schmidt, J. 2016, "Industrial silicon solar cells applying the Passivated Emitter and Rear Cell (PERC) concept—A review", *IEEE J. Photovolt.,* Vol. 6, pp. 1366–1381.
[39] Dullweber, T. et al. 2018, "Present status and future perspectives of bifacial PERC+ solar cells and modules", *Jpn. J. Appl. Phys.,* Vol. 57, 08RA01.
[40] Brendel, R. 2012, "Modeling solar cells with the dopant-diffused layers treated as conductive boundaries", *Prog. Photovolt: Res. Appl.,* Vol. 20, pp. 31–43.
[41] Fell, A. 2013, "A free and fast three-dimensional/two-dimensional solar cell simulator featuring conductive boundary and quasi-neutrality approximations", *IEEE Trans. Electron Dev.,* Vol. 60, pp. 733–738.
[42] Reiter, S. et al. 2016, "Parasitic absorption in polycrystalline Si-layers for carrier-selective front junctions", *Energy Procedia*, Vol. 92, pp. 199–204.
[43] Min, B. et al. 2018, "Increasing the photo-generated current in solar cells with passivating contacts by reducing the poly-Si deposition temperature", *AIP Conf. Proc.*, Vol. 1999, 040015.

About the Authors

Dr. Thorsten Dullweber leads the industrial solar cells R&D group at ISFH. His research work focuses on high-efficiency industrial-type PERC and PERC+ silicon solar cells and ultrafine-line screen-printed Ag front contacts. Before joining ISFH in 2009, he spent nine years as a project leader in the microelectronics industry at Siemens AG and later worked for Infineon Technologies AG.

Dr. Robby Peibst obtained his diploma degree in technical physics in 2005. In 2010 he received his Ph.D. from the Leibniz University of Hanover, with a thesis on germanium-nanocrystal-based memory devices. He joined ISFH in 2010 and has led the emerging solar technologies group since 2013. His research focuses on the development of techniques for enabling the production of high-efficiency silicon solar cells.

Rolf Brendel is the scientific director of ISFH. He received his Ph.D. in materials science from the University of Erlangen, for which he researched infrared spectroscopy. In 2004 he joined the Institute of Solid State Physics of the Leibniz University of Hanover as a full professor. His main research focuses on the physics and technology of crystalline silicon solar cells.

Enquiries

Institute for Solar Energy Research Hamelin (ISFH)
Am Ohrberg 1
31860 Emmerthal
Germany

Email: dullweber@isfh.de
Tel: +49-5151-999-642